(36) Zimm, B. H. *J. Chem. Phys.* **1948**, *16*, 1093.
(37) Evans, J. M. In *Light Scattering from Polymer Solutions*; Huglin, M. B., Ed.; Academic: New York, 1972; Chapter 5.
(38) Siano, D. B.; Applequist, J. *Macromolecules* **1975**, *8*, 858.
(39) Casassa, E. F.; Eisenberg, H. *Adv. Protein Chem.* **1964**, *19*, 287.
(40) Strazielle, C. In *Light Scattering from Polymer Solutions*; Huglin, M. B., Ed.; Academic: New York, 1972; Chapter 15.
(41) Kruis, A. *Z. Phys. Chem.* **1936**, *34B*, 13.
(42) Meyer, R. J., Ed. *Gmelins Handbuch der Anorganischen Chemie, Natrium*; Verlag Chemie GMBH: Berlin, 1928; Vol. 21, p 349.
(43) Johnson, B. L.; Smith, J. In *Light Scattering from Polymer Solutions*; Huglin, M. B., Ed.; Academic: New York, 1972; Chapter 2.
(44) Weast, R. C., Ed. *CRC Handbook of Chemistry and Physics*, 58th ed.; CRC Press: Cleveland, OH, 1977; p E-223.
(45) Ehl, J.; Loucheux, C.; Reiss, C.; Benoit, H. *Makromol. Chem.* **1964**, *75*, 35.
(46) Eisenberg, H.; Felsenfield, G. *J. Mol. Biol.* **1967**, *30*, 17.
(47) Utiyama, H. In *Light Scattering from Polymer Solutions*; Huglin, M. B., Ed.; Academic: New York, 1972; Chapter 4.
(48) Okuyama, K.; Arnott, S.; Moorhouse, R.; Walkinshaw, M. D.; Atkins, E. D. T.; Wolf-Ullish, Ch. In *Fiber Diffraction Methods*; French, A. D., Gardner, K. N., Eds.; American Chemical Society: Washington, DC, 1980; Chapter 26, ACS Symp. Ser., No. 141.
(49) Shibata, J. H.; Schurr, J. M. *Biopolymers* **1981**, *20*, 525.
(50) Applequist, J.; Damle, V. *J. Am. Chem. Soc.* **1965**, *82*, 1450.
(51) Washington, G. E.; Brant, D. A., manuscript in preparation.
(52) Pérez, S.; Vergelati, C. *Int. J. Biol. Macromol.*, in press.
(53) Elias, H.-G.; Bareiss, R.; Watterson, J. G. *Adv. Polym. Sci.* **1973**, *11*, 111.
(54) Tanford, C. *Physical Chemistry of Macromolecules*; Wiley: New York, 1961; Chapter 4.
(55) Devore, D. I.; Manning, G. S. *Biophys. Chem.* **1974**, *2*, 42.
(56) Manning, G. S. *Q. Rev. Biophys.* **1978**, *11*, 179.
(57) Hacche, L. S. Ph.D. Dissertation, University of California, Irvine, 1986.
(58) Elias, H.-G. In *Light Scattering from Polymer Solutions*; Huglin, M. B., Ed.; Academic: New York, 1972; Chapter 9.
(59) Odijk, T.; Houwaart, A. C. *J. Polym. Sci., Polym. Phys. Ed.* **1978**, *16*, 627.

Use of Multidetector Light-Scattering Experiments To Study the Flexibility of Individual Polymer Chains in Solution

William G. Griffin,* Mary C. A. Griffin,† and François Boué‡

EMRI, Brunel University, Egham, Surrey TW20 0JZ, UK, AFRC Institute of Food Research, Reading Laboratory, Shinfield, 0HE, RG2 9AT, UK, and TCM Group, Cavendish Laboratory, Cambridge CB3 0HE, UK. *Received December 24, 1986*

ABSTRACT: A general expression for the four-particle electric field amplitude correlation function for light scattered by Gaussian polymer chains is given and used to evaluate the intensity cross-correlation function measured in a two-detector dynamic light-scattering experiment for flexible (Rouse) and semiflexible (Harris–Hearst) polymer chains. The results are compared with those for a rigid-rod scatterer, and the possibility of using two-detector, cross-correlation techniques to distinguish between rigid, semiflexible, and flexible polymers is discussed. A procedure for approximating the four-particle function for a Gaussian chain is given with a numerical example of the time-dependent contribution of the first mode of a Rouse chain to the decay of the intensity correlations. For the Rouse chain the time dependence of the cross-correlation function exhibits a $(kR_g)^2$ dependence on the scattering vector for $\mathbf{k}_1 \cong \mathbf{k}_2$ and $kR_g \gtrsim 4$.

Introduction

Conventional, single-detector, dynamic light-scattering techniques can be used to measure internal relaxations of flexible polymers in solution. Examples of such experiments are studies of DNA[1] and F actin.[2] The correlation of intensity fluctuations is measured, and, for large numbers of scatterers in the scattering volume, this intensity correlation is related to the electric field correlations by the Siegert relation.[3] Theories of polymer dynamics can be used to calculate the time dependence of the field correlation function, $g^{(1)}(\mathbf{k},t) \propto \langle E^*(\mathbf{k},0)E(\mathbf{k},t)\rangle$; for example, $g^{(1)}$ was calculated for the Rouse model by Pecora[4] and for a semiflexible chain model by Maeda and Fujime.[5] Those authors also calculated the Fourier Transform of $g^{(1)}$, which is related to the spectral distribution of the scattered light. In the present work we report results for field and intensity correlations which can be directly measured by digital correlation techniques. The electric field correlation function, $g^{(1)}(\mathbf{k},t)$, is strongly affected by the translational diffusive motion of the polymer molecules. For polarized light scattering, length and time scales of internal modes are in principle measurable for $kR_g > 1$, provided the contribution of the translational motion to $g^{(1)}(\mathbf{k},t)$ can be accurately allowed for. Such investigations offer technical problems[5,6,7] as the center-of-mass motion of the macromolecule must be accurately characterized independently of any intramolecular effects. Only then can the contribution of the center-of-mass diffusion to the time dependence of the intensity correlation function be eliminated to obtain the intramolecular time-dependent contribution. It is therefore of value to devise quasi-elastic light-scattering experiments in which the contribution of the center-of-mass motion to the observed correlations is eliminated or reduced.

The particular type of dynamic light-scattering experiment to be discussed in this paper involves the use of two (or more) photomultipliers set up to receive the light scattered by individual macromolecules passing through the same small scattering volume; the photomultiplier outputs are cross correlated (see Figure 1). The feasibility of such experiments was established by Griffin and Pusey,[8] who predicted and observed an anticorrelation in the intensity cross-correlation function, $g^{(2)}(\mathbf{k}_1,\mathbf{k}_2;t)$, $(\mathbf{k}_1\cdot\mathbf{k}_2 = 0)$, for light scattered by rotating rodlike scatterers. The theoretical results given here apply over the experimentally accessible range of both scattering vectors: thus they apply

*To whom all correspondence should be addressed at Brunel University.
†AFRC Institute of Food Research.
‡TCM Group. Present address: Centre d'Etudes Nucléaires de Saclay, Gif-Sur-Yvette, France.

0024-9297/87/2220-2187$01.50/0

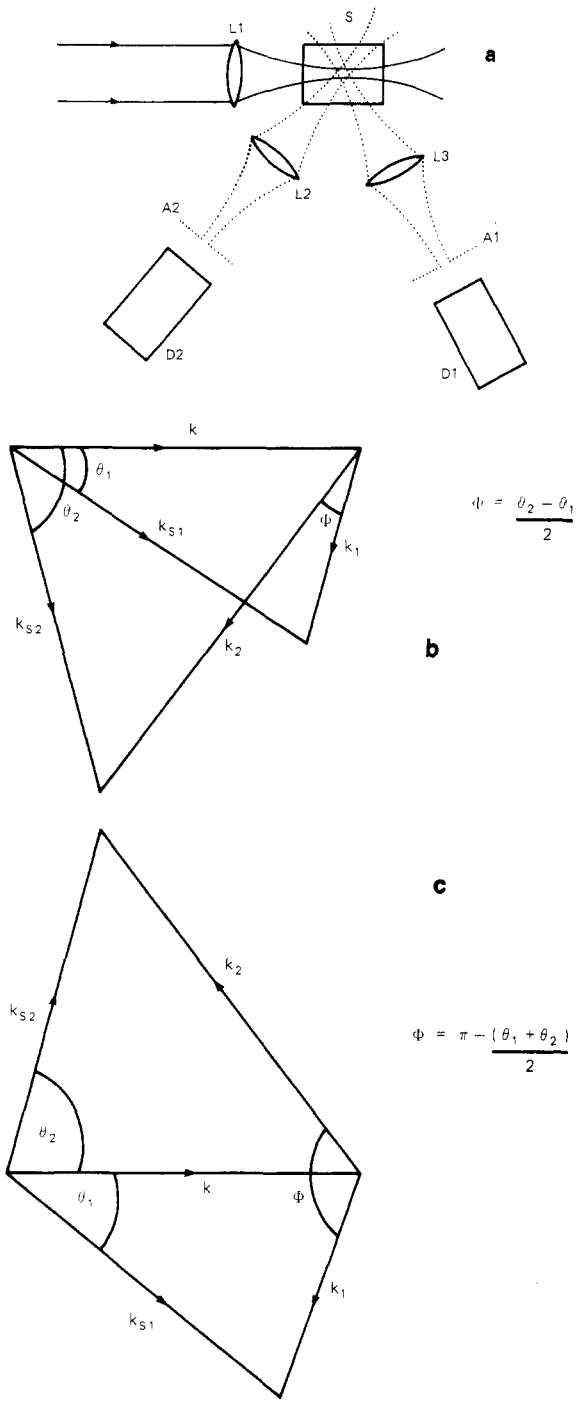

Figure 1. (a) Photon cross-correlation experiment. Laser light is focused through lens L1 into the sample cell S. Two similar lenses (L2 and L3) cast images of the focal region onto apertures A1 and A2 in front of two photodetectors D1 and D2, which are positioned at scattering angles θ_1 and θ_2. The outputs of D1 and D2 are cross correlated. (b and c) Two scattering vector geometries for this experiment. In (b) the detectors are on the same side while in (c) they are on opposite sides of the laser beam.

to experiments such as those of Kam and Rigler[9] in which the two detectors were nearly superimposed.

Pusey[10] has recently presented a description of the problem to be tackled in calculating the photon cross-correlation function for a Gaussian coil, using the Rouse model, and has given an expression for the static part, $g^{(2)}(\mathbf{k}_1,\mathbf{k}_2;0)$. In the method given here $g^{(2)}(\mathbf{k}_1,\mathbf{k}_2;t)$ is expressed in terms of the normal modes of the polymer chain; the relaxation times of the modes determine the dependence of $g^{(2)}$ on time. Numerical and analytical results are presented for models of flexible polymers and numerical results are given for semiflexible polymers. A comparison of $g^{(2)}$ for rodlike scatterers with $g^{(2)}$ for semiflexible polymers is presented.

Theory

The intensity cross-correlation function measured in a two-detector experiment, in the case of dilute suspensions and small scattering volume, V, is given by[11]

$$g^{(2)}(\mathbf{k}_1,\mathbf{k}_2;t) = \frac{\langle I(\mathbf{k}_1,0)I(\mathbf{k}_2,t)\rangle}{\langle I(\mathbf{k}_1)\rangle\langle I(\mathbf{k}_2)\rangle}$$

$$= 1 + |g_{\mathrm{INT}}^{(1)}(\mathbf{k},t)|^2 + g_{\mathrm{NG}}^{(2)}(\mathbf{k},t); \qquad \mathbf{k}_1 = \mathbf{k}_2 = \mathbf{k} \tag{1a}$$

$$= 1 + g_{\mathrm{NG}}^{(2)}(\mathbf{k}_1,\mathbf{k}_2;t); \qquad \mathbf{k}_1 \neq \mathbf{k}_2 \tag{1b}$$

where $\mathbf{k}_1$ and $\mathbf{k}_2$ are the scattering vectors corresponding to the two detector positions, $g_{\mathrm{INT}}^{(1)}$ is the interference term and $g_{\mathrm{NG}}^{(2)}$ is the four-particle (cross)-correlation function. (Strictly, eq 1b is an approximation, but the error is negligible provided $|\mathbf{k}_1 - \mathbf{k}_2|V^{1/3} \gg 1$.) The latter, non-Gaussian, term can be factorized into a number fluctuation term, $g_{\mathrm{NG}}^{(2)T}$ arising from the translational diffusion of the scatterers in and out of the scattering volume and an intramolecular term, $g_{\mathrm{NG}}^{(2)I}$, which we now proceed to analyze. The number fluctuation term can be calculated explicitly and used to extract the intramolecular term from the experimental data.

We define the four-particle scattering function to be

$$g_{\mathrm{NG}}^{(2)I}(\mathbf{k}_1,\mathbf{k}_2;t) = [\sum_{ijkl}\langle \exp[i\mathbf{k}_1\cdot[\mathbf{r}_i(0) - \mathbf{r}_j(0)] + i\mathbf{k}_2\cdot [\mathbf{r}_k(t) - \mathbf{r}_l(t)]]\rangle]/[\sum_{ij}\langle \exp[i\mathbf{k}_1\cdot[\mathbf{r}_i(0) - \mathbf{r}_j(0)]]\rangle \sum_{ij}\langle \exp[i\mathbf{k}_2\cdot [\mathbf{r}_i(0) - \mathbf{r}_j(0)]]\rangle] \tag{2}$$

where $\mathbf{r}_i$ is the position vector of the ith segment of an individual polymer molecule.

We now consider the cases of a rigid rod and a Gaussian chain.

Four-Particle Correlation Function for Rigid Rods. For the purposes of comparison we recall the form of $g^{(2)}$ for a rigid-rod scatterer. As has been shown elsewhere,[8] the four-particle correlation function of such a scatterer has the form:

$$g_{\mathrm{NG}}^{(2)I}(\mathbf{k}_1,\mathbf{k}_2;t) = \mathcal{N}^{-1}\sum_{l,\ \mathrm{even}}(2l+1)P_l(\hat{\mathbf{k}}_1\cdot\hat{\mathbf{k}}_2)e^{-l(l+1)D_R t}\Lambda_l(k_1,k_2) \tag{3}$$

where the P_l are Legendre polynomials of order l, $\mathcal{N}$ is a normalization (we use $\mathcal{N}$ for different normalization constants elsewhere; no confusion can arise) given by

$$\mathcal{N} = \langle I(\mathbf{k}_1)\rangle\langle I(\mathbf{k}_2)\rangle \tag{4}$$

and Λ_l is given by

$$\Lambda_l(k_1,k_2) = \sum_{\substack{pp'qq' \\ \text{even}}}\sum (i)^{p+q-p'-q'}(2p+1)(2p'+1)(2q+1)(2q'+1)\times I_{pp'}(k_1)I_{qq'}(k_2)\begin{pmatrix} l & p & p' \\ 0 & 0 & 0\end{pmatrix}^2\begin{pmatrix} l & q & q' \\ 0 & 0 & 0\end{pmatrix}^2 \tag{5}$$

with

$$I_{pp'}(k) = (2/kL)^2\int_0^{kL/2}dx_1\int_0^{kL/2}dx_2\, j_p(x_1)j_{p'}(x_2) \tag{6}$$

where D_R is the rotational diffusion coefficient of a rod of length L and j_p is the spherical Bessel function of order p.

Four-Particle Correlation Function for Gaussian Chains. A Gaussian, Markov polymer chain is made up of linked segments such that the mean-squared distance between segments m links apart is proportional to m, i.e.,

$$\langle r^2(m)\rangle = l^2 m \tag{7}$$

where l is defined as the statistical segment length, while the probability of any two segments being separated by a distance r is given by a Gaussian distribution.[12] For a Gaussian chain with linear dynamical equations our result for $g_{NG}^{(2)I}$ can be expressed in terms of the normal modes $\{\mu_\alpha\}$ of the chain as

$$g_{NG}^{(2)I}(\mathbf{k}_1,\mathbf{k}_2;t) = \left[\sum_{ijkl}\prod_{\alpha}\exp\left[-\frac{\langle\mu_\alpha^2\rangle}{6}(k_1^2Q_{ij\alpha}^2 + k_2^2Q_{kl\alpha}^2) - \frac{\langle\mu_\alpha^2\rangle}{3}\mathbf{k}_1\cdot\mathbf{k}_2Q_{ij\alpha}Q_{kl\alpha}e^{-t/\tau_\alpha}\right]\right] \Big/ \left[\left[\sum_{ij}\prod_{\alpha}\exp\left(-\frac{\langle\mu_\alpha^2\rangle}{6}k_1^2Q_{ij\alpha}^2\right)\right]\times\left[\sum_{ij}\prod_{\alpha}\exp\left(-\frac{\langle\mu_\alpha^2\rangle}{6}k_2^2Q_{ij\alpha}^2\right)\right]\right] \tag{8}$$

where the coordinates of the "beads" are given by

$$\mathbf{r}_i = \sum_{\alpha=1}^{N} Q_{i\alpha}\mu_\alpha \tag{9}$$

the $\langle\mu_\alpha^2\rangle$ are the mean-square equilibrium mode lengths, the τ_α are the corresponding relaxation times and the condensed notation

$$Q_{ij\alpha} = Q_{i\alpha} - Q_{j\alpha} \tag{10}$$

has been used.

(a) The Rouse Model for a Flexible Polymer. For the case of a flexible polymer, Rouse chain dynamics can be conveniently described by a Smoluchowski equation

$$\frac{\partial\psi}{\partial t} = \sum_{\alpha=0}^{N}\frac{1}{\tau_\alpha}[(\langle\mu_\alpha^2\rangle/3)\nabla_\alpha^2\psi + \nabla_\alpha\cdot(\psi\mu_\alpha)] \tag{11}$$

where ψ is the chain position distribution function. [Zwanzig[13] gives an equivalent Langevin description of the Rouse–Zimm chain. Further on we use a Langevin description for the Harris–Hearst model of a semiflexible chain, but the key assumption we make for both Rouse–Zimm and Harris–Hearst models is that the chains can be described by Gaussian chains. The exact solution of eq 11 for the Rouse chain describes an ideal Gaussian chain exactly. For the Harris–Hearst model, the canonical distribution of "bead" positions and momenta is given by Harris and Hearst in Gaussian form to reflect the linearity of their defining equation of motion for the chain. Soda[14] proposed a nonlinear dynamical equation for a semiflexible chain based on the model of Harris and Hearst; the Harris–Hearst equation of motion is shown by Soda to be a linearization of this equation which is not self-consistent. In the rigid limit of such a model a Gaussian distribution for the bond probabilities[12] is not appropriate, but, for small degrees of rigidity, such a representation may be valid (see Moro and Pecora[15]). Our results (see below) support the general conclusion of these authors that the flexible limit of the Harris–Hearst model provides a correct representation of the Rouse chain.] We adopt the notation used by Pecora[16] and Verdier and Stockmayer.[17] The solution to eq 11 in terms of normal modes of the polymer chain is known.[18] For the Rouse chain we have

$$\langle\mu_\alpha^2\rangle = \frac{b^2N^2}{\pi^2\alpha^2} \tag{12}$$

and

$$\tau_\alpha = \frac{b^2N^2\zeta}{3\pi^2\alpha^2k_BT} \tag{13}$$

where b is the mean distance between beads, N is the number of beads, ζ is the bead friction coefficient, k_B is the Boltzmann constant, T is the absolute temperature, and for Rouse polymer chains the $Q_{i\alpha}$ are given by

$$Q_{i\alpha} = \left(\frac{2}{N}\right)^{1/2}\cos\pi\alpha\left(\frac{i}{N}-\frac{1}{2}\right) \qquad \alpha \text{ even}$$

$$Q_{i\alpha} = \left(\frac{2}{N}\right)^{1/2}\sin\pi\alpha\left(\frac{i}{N}-\frac{1}{2}\right) \qquad \alpha \text{ odd} \tag{14}$$

The exact solution to eq 11 is used to calculate an analytical expression for $g_{NG}^{(2)I}$ in the form of eq 8 in terms of the quantities defined above. In the continuum limit this takes the form

$$g_{NG}^{(2)I}(\mathbf{k}_1,\mathbf{k}_2;t) = \mathcal{N}^{-1}\int_0^N\int_0^N\int_0^N\int_0^N \exp\left[-\left[\frac{b^2k_1^2}{6}|i-j| + \frac{b^2k_2^2}{6}|k-l| + \frac{\mathbf{k}_1\cdot\mathbf{k}_2}{6}b^2(|i-l| + |j-k| - |i-k| - |j-l|)e^{-t/\tau_\alpha}\right]\right] di\,dj\,dk\,dl \tag{15}$$

where $\mathcal{N}$ is a normalization constant given by

$$\mathcal{N} = \int_0^N\int_0^N \exp\left[-\left(\frac{b^2k_1^2}{6}|i-j|\right)\right] di\,dj \times \int_0^N\int_0^N \exp\left[-\left(\frac{b^2k_2^2}{6}|i-j|\right)\right] di\,dj \tag{16}$$

This is straightforward to evaluate at $t = 0$ by elementary techniques. (We obtain the same result as reported recently by Pusey[10] after correcting a small error in his result.[19]) All higher order correlations can also be calculated exactly.[20]

For sufficiently small k_1R_g and k_2R_g the time dependence of $g_{NG}^{(2)I}$ can be evaluated analytically by expansion of the exponential of the time-dependent factor of eq 8 as

$$g_{NG}^{(2)I} = \mathcal{N}^{-1}\sum_{ijkl}\prod_{\alpha}\exp\left[-\frac{\langle\mu_\alpha^2\rangle}{6}(k_1^2Q_{ij\alpha}^2 + k_2^2Q_{kl\alpha}^2)\right]\left[\sum_{n=0}^{\infty}\frac{(-)^n}{n!}\left(\sum_{\alpha}\frac{\mathbf{k}_1\cdot\mathbf{k}_2}{3}\langle\mu_\alpha^2\rangle Q_{ij\alpha}Q_{kl\alpha}e^{-t/\tau_\alpha}\right)^n\right] \tag{17}$$

where the normalization is given by

$$\mathcal{N} = \sum_{ij}\prod_{\alpha}\exp\left(-\frac{\langle\mu_\alpha^2\rangle}{6}k_1^2Q_{ij\alpha}^2\right)\sum_{ij}\prod_{\alpha}\exp\left(-\frac{\langle\mu_\alpha^2\rangle}{6}k_2^2Q_{ij\alpha}^2\right) \tag{18}$$

The first two nonvanishing terms can be written

$$g_{NG}^{(2)I} \cong 1 + \mathcal{N}^{-1}\frac{(\mathbf{k}_1\cdot\mathbf{k}_2)^2}{18}\sum_{\alpha\alpha'}\langle\mu_\alpha^2\rangle\langle\mu_{\alpha'}^2\rangle\Psi_{\alpha\alpha'}(k_1)\Psi_{\alpha\alpha'}(k_2)e^{-t[(1/\tau_\alpha)+(1/\tau_{\alpha'})]} \tag{19}$$

where $\Psi_{\alpha\alpha'}$ is defined as

$$\Psi_{\alpha\alpha'}(k) = \sum_{ij} \exp\left(-\sum_{\alpha} \frac{\langle \mu_\alpha^2 \rangle}{6} k^2 Q_{ij\alpha}^2 \right) Q_{ij\alpha} Q_{ij\alpha'} \quad (20)$$

For larger values of $k_1 R_g$ and $k_2 R_g$ eq 8 has been evaluated numerically, as described later, making use of the relationship

$$R_g^2 = Nb^2/6 \quad (21)$$

(b) The Harris–Hearst Model for Semiflexible Polymers. In this model[21] the polymer is described as a wormlike chain with both longitudinal elasticity and bending elasticity.[14,15] The Langevin equation for this model is

$$\rho \frac{\partial^2 \mathbf{r}}{\partial t^2} + \zeta' \frac{\partial \mathbf{r}}{\partial t} + \epsilon \frac{\partial^4 \mathbf{r}}{\partial s^4} - \kappa \frac{\partial^2 \mathbf{r}}{\partial s^2} = \mathbf{A}(s,t) \quad (22)$$

where ρ is the linear mass density, ζ' is the friction constant per unit length, $\mathbf{A}(s,t)$ is the random Brownian force, and ϵ and κ are respectively the bending and elongational elastic constants. The polymer is described by the curve $\mathbf{r} = \mathbf{r}(s,t)$ where s gives the position along the chain. This model incorporates the following assumptions: (i) that

$$\left(\frac{\partial^2 \mathbf{r}}{\partial s^2} \right)^2 \gg \left(\frac{\partial^2 \mathbf{r}}{\partial s^2} \cdot \hat{\mathbf{e}} \right)^2 \quad (23)$$

where $\hat{\mathbf{e}}$ is a unit vector pointing in the direction of the tangent to the chain at given s and t and (ii) that

$$(|\partial \mathbf{r}/\partial s| - 1)^2 \cong [\partial \mathbf{r}/\partial s]^2 \quad (24)$$

As discussed by Soda,[14] these two assumptions are, in fact, mutually incompatible, but Moro and Pecora[15] and Hearst and Harris[22] have suggested that, nevertheless, the model gives a reasonable description of polymers with small rigidity. Furthermore, the numerical results of Hearst et al.[23] show that, for flexibilities intermediate between rod and coil limits, major differences between $\langle [\mathbf{r}(s) - \mathbf{r}(s')]^2 \rangle$ for the Harris–Hearst and Kratky–Porod models occur only for values of s close to s' and at the ends of the chain. Moro and Pecora[15] gave solutions to eq 22, expanding $\mathbf{r}(s,t)$ and $\mathbf{A}(s,t)$ in terms of a complete, orthonormal set of functions, $\{q_l\}$:

$$\mathbf{r}(s,t) = \sum_l \mathbf{p}_l(t) q_l(s) \quad (25)$$

and

$$\mathbf{A}(s,t) = \sum_l \mathbf{B}_l(t) q_l(s) \quad (26)$$

The lth normalized eigenfunction was obtained from the eigenvalue equation

$$\epsilon \frac{\mathrm{d}^4 q_l(s)}{\mathrm{d}s^4} - \kappa \frac{\mathrm{d}^2 q_l(s)}{\mathrm{d}s^2} = \lambda_l q_l(s) \quad (27)$$

as

$$q_l(s) = C_l \Bigg[\cos \nu_{2l} s + (\nu_{2l}/\nu_{1l})^2 \cosh \nu_{1l} s + \frac{\sin \nu_{2l} L + (\nu_{2l}/\nu_{1l})^3 \sinh \nu_{1l} L}{\cos \nu_{2l} L - \cosh \nu_{1l} L} [\sin \nu_{2l} s + (\nu_{1l}/\nu_{2l}) \sinh \nu_{1l} s] \Bigg] \quad (28)$$

where C_l is a normalization constant, L is the polymer length, and ν_{1l} and ν_{2l} are defined as

$$\nu_{1l} = \left[\left[\left(\frac{\kappa}{2\epsilon} \right)^2 + \frac{\lambda_l}{\epsilon} \right]^{1/2} + \frac{\kappa}{2\epsilon} \right]^{1/2} \quad (29)$$

and

$$\nu_{2l} = \left[\left[\left(\frac{\kappa}{2\epsilon} \right)^2 + \frac{\lambda_l}{\epsilon} \right]^{1/2} - \frac{\kappa}{2\epsilon} \right]^{1/2}$$

The eigenvalues, $\{\lambda_l\}$, are obtained by solving

$$2(1 - \cosh \nu_{1l} L \cos \nu_{2l} L) = \left[\left(\frac{\nu_{1l}}{\nu_{2l}} \right)^3 - \left(\frac{\nu_{2l}}{\nu_{1l}} \right)^3 \right] \sinh \nu_{1l} L \sin \nu_{2l} L \quad (30)$$

Following the treatment of Moro and Pecora[15] we introduce the scaled parameters $\kappa^* = \kappa/L^2$ and $\epsilon^* = \epsilon/L^4$ and express the "stiffness" of the polymer in terms of the dimensionless parameter ϵ^*/κ^*. The eigenvalues can be expressed in terms of the dimensionless parameter, $x_l = \lambda_l L^2/\kappa$ and have been obtained by searching for minima[24] of the square of the difference between the right- and left-hand sides of eq 30 (typically, the relative error was less than 10^{-7}) in a series of finite intervals chosen by successive subdivision so as to obtain all the eigenvalues. Table I gives the values of x_l for the first 10 eigenfunctions for a range of values of ϵ^*/κ^* that have been used in this work.

The elastic constants, ϵ and κ, have been given in terms of γ, the inverse of the statistical length, as[25]

$$\epsilon = 3kT/4\gamma \text{ and } \kappa = 3k_B T \gamma \mu(\gamma L) \quad (31)$$

where

$$\mu(\gamma L) = [1 - (1 - e^{-2\gamma L})/2\gamma L]^{-1} \quad (32)$$

Thus,

$$\mu(\gamma L)(2\gamma L)^2(\epsilon^*/\kappa^*) = 1 \quad (33)$$

For each given value of ϵ^*/κ^* and L the value of γ was obtained by minimizing[24] the square of the difference between the left- and right-hand sides of eq 33 (typically, the relative error was less than 10^{-6}). Values for γL, the number of statistical segments in the polymer, and the ratio L/R_g are plotted against ϵ^*/κ^* in Figure 2.

Assuming that the chains obey Gaussian statistics, we have substituted the expressions for $q_\alpha(i)$ as $Q_{i\alpha}$ in eq 8. To ensure equipartition of energy, we must have

$$\langle \mu_\alpha^2 \rangle = 3k_B T/\lambda_\alpha \quad (34)$$

and we also require that

$$\tau_\alpha = \zeta'/\lambda_\alpha \quad (35)$$

The mean-square radius of gyration is given by

$$\langle R_g^2 \rangle = \frac{3k_B T}{L} \sum_l \frac{1}{\lambda_l} \quad (36)$$

It should be pointed out that in this model the quantities represented by $q_\alpha(i)$ and $\langle \mu_\alpha^2 \rangle$ are not directly comparable with those for the Rouse model. Here, $q_\alpha(i)$ has dimensions of $L^{-1/2}$, and $\langle \mu_\alpha^2 \rangle$ of L^3, while in the Rouse model $Q_{i\alpha}$ is dimensionless and $\langle \mu_\alpha^2 \rangle$ has dimensions of L^2.

Numerical Evaluation of Equation 8. Three different quadrature routines from the NAG software library were used to perform quadrature in two and four dimensions on a VAX 11/750 computer. These were (i) an adaptive Monte-Carlo routine,[26] (ii) an adaptive deterministic routine,[27] and (iii) a routine using a product of Gaussian rules.[28] All these routines gave answers in good agreement with one another, but the last routine, which

Table I
Values of x_l

l	ϵ^*/κ^* = 0.001[a]	0.01	0.1	1[a]	1000[a]
1	9.954 659 1 × 10^0	1.046 073 2 × 10^1	1.155 015 9 × 10^1	1.194 435 7 × 10^1	1.199 994 3 × 10^1
2	4.083 788 1 × 10^1	4.919 483 7 × 10^1	9.852 820 3 × 10^1	5.499 339 9 × 10^2	5.006 133 8 × 10^5
3	9.569 935 6 × 10^1	1.400 074 2 × 10^2	4.884 497 9 × 10^2	3.912 382 9 × 10^3	3.803 646 0 × 10^6
4	1.796 082 3 × 10^2	3.274 154 6 × 10^2	1.648 200 9 × 10^3	1.480 445 9 × 10^4	1.461 781 7 × 10^7
5	2.996 662 2 × 10^2	6.799 341 8 × 10^2	4.278 800 7 × 10^3	4.022 845 9 × 10^4	3.994 408 4 × 10^7
6	4.650 616 8 × 10^2	1.290 544 4 × 10^3	9.315 594 7 × 10^3	8.953 762 0 × 10^4	8.913 581 0 × 10^7
7	6.871 577 5 × 10^2	2.276 102 6 × 10^3	3.151 729 0 × 10^4	1.744 208 2 × 10^5	1.738 818 5 × 10^8
8	9.795 900 2 × 10^2	3.776 960 6 × 10^3	5.172 138 4 × 10^4	3.089 049 8 × 10^5	3.082 091 5 × 10^8
9	1.358 347 2 × 10^3	5.956 846 1 × 10^3	1.196 873 6 × 10^5	5.093 548 4 × 10^5	5.084 824 2 × 10^8
10	1.841 820 4 × 10^3	1.312 538 9 × 10^4	1.718 911 0 × 10^5	7.944 729 3 × 10^5	7.934 042 0 × 10^8

[a] Values in agreement with those given by Moro and Pecora.[15]

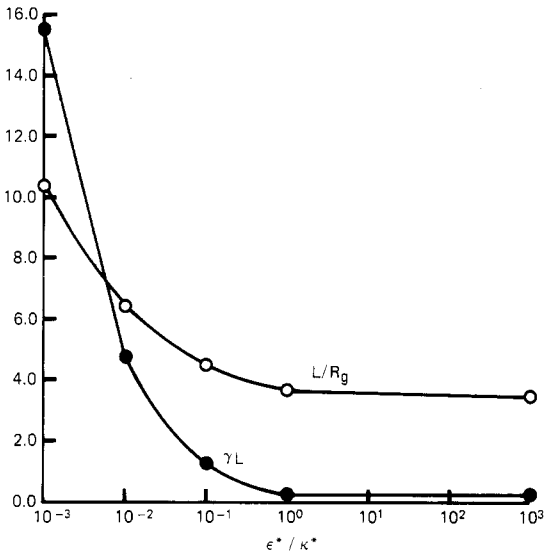

Figure 2. Number of statistical lengths, γL (●), and the ratio of polymer chain length, L, to its radius of gyration, R_g (○), shown as functions of the stiffness parameter, ϵ^*/κ^*.

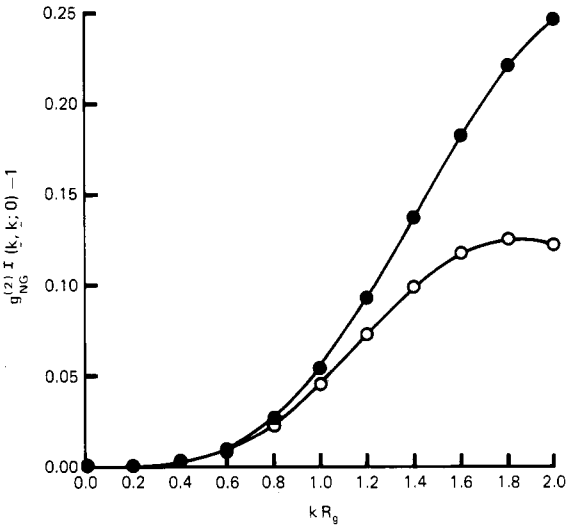

Figure 3. $g_{NG}^{(2)I}(0)$ for the geometry of Figure 1c for $|\mathbf{k}_1| = |\mathbf{k}_2|$, R_g = 300 nm, and λ = 451 nm, plotted against kR_g: (○) Shows results from the series expansion (eq 19) and (●) from numerical quadrature of eq 8.

involved evaluation of the integrand over a grid in two- and four-dimensional space, was consistently more accurate than the Monte-Carlo routine and ran more quickly than the adaptive routine for the same level of accuracy. The numerical results actually described here are therefore derived from this routine. For each set of input values ($\mathbf{k}_1$, $\mathbf{k}_2$, the wavelength, λ, of the incident light, R_g, and ζ for the Rouse model; $\mathbf{k}_1$, $\mathbf{k}_2$, λ, ϵ^*/κ^*, and ζ' for the Harris–Hearst model) the number of modes included and the total number of points in the two- or four-dimensional grid was increased steadily. A final value for $g_{NG}^{(2)I}(\mathbf{k}_1,\mathbf{k}_2;t)$ was taken when there were no further significant changes in the numerator or denominator of eq 8. Results are given here for ζ' = 0.001 N·s and for ζ adjusted so that τ_1 for the Rouse model is equal to τ_1 for the Harris–Hearst model when ϵ^*/κ^* = 0.001. At high kR_g (>5) the CPU time required for each evaluation was very long (20–36 h); fewer calculations, therefore, were completed in this region.

Results and Discussion

Some checks were made on the computer programs as follows. First of all, for scattering vectors perpendicular to one another ($\mathbf{k}_1\cdot\mathbf{k}_2 = 0$), $g_{NG}^{(2)I}(\mathbf{k}_1,\mathbf{k}_2;0)$ was found to be unity from the programs written for both the Rouse and the Harris–Hearst models. This property of eq 8 is true for Gaussian chains; i.e., it is true exactly for the Rouse and Rouse–Zimm models and approximately true for the Harris–Hearst model in the limit of high flexibility.[15] Second, values obtained numerically for $g_{NG}^{(2)I}(0)$ for the Rouse model were in agreement with those obtained analytically. It was also found that the sign of $\mathbf{k}_1\cdot\mathbf{k}_2$ could be reversed in eq 8 without altering the value obtained for $g_{NG}^{(2)I}$. This property is reflected in the symmetry of eq 3.8 of Pusey[10] under substitution of W by $-W$.

The function Ψ_{11} in eq 20 has been evaluated analytically and used to estimate $g_{NG}^{(2)I}(0)$ for a Rouse-type random coil with $|\mathbf{k}_1| = |\mathbf{k}_2|$, R_g = 300 nm, λ = 451 nm, and $0.2 \leq kR_g \leq 2.0$. (It is worth noting that in the case where $\mathbf{k}_1 \neq \mathbf{k}_2$, Φ, and hence $g_{NG}^{(2)I}$, are functions of R_g and of the wavelength of incident light.) These results are compared in Figure 3 with results obtained by numerical quadrature from eq 8. As kR_g increases, the approximate value of $g_{NG}^{(2)I}(0) - 1$ obtained from eq 19 diverges from the more exact values derived from eq 8; however, at kR_g = 1.2 they agree to within 21%. Figure 4 shows $g^{(2)}(t) - 1 = g_{NG}^{(2)T}(t)g_{NG}^{(2)I}(t)$ plotted against time for $k_1R_g = k_2R_g$ = 1.2, where the α = 1 mode dominates the time-dependent part of $g_{NG}^{(2)I}$; $g_{NG}^{(2)I}$ has been estimated by using eq 19. As discussed later, for k_1R_g, $k_2R_g \gg 1$, several low-order modes contribute to the time dependence, resulting in a complex multiexponential time dependence for $g_{NG}^{(2)I}$.

In order to simplify the discussion, we refer in all that follows only to results obtained by numerical quadrature of eq 8.

Figure 5 shows $g_{NG}^{(2)I}(\mathbf{k}_1,\mathbf{k}_2;0)$ plotted in isometric projection calculated for a polymer with R_g = 193.3 nm and λ = 451 nm for the range of values $0 \leq k_1R_g \leq 2.5$, $0 \leq k_2R_g \leq 2.5$ for the Rouse model and for a very flexible polymer of the Harris–Hearst type ($\epsilon^*/\kappa^* = 0.001$). Results for the

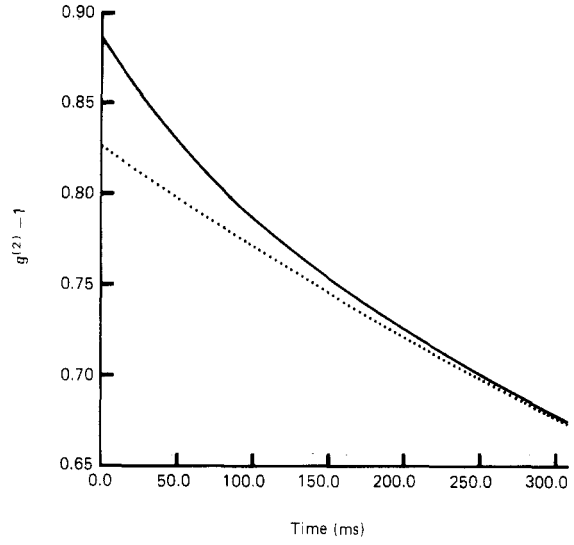

Figure 4. Intensity cross-correlation function calculated from the series expansion (eq 19) vs. delay time in milliseconds for the geometry of Figure 1c and $|\mathbf{k}_1| = |\mathbf{k}_2|$, $k_1R_g = k_2R_g = 1.2$, $R_g = 300$ nm, and $\lambda = 451$ nm: (—) $(g^{(2)}(t) - 1) = g_{NG}{}^{(2)T}(t)g_{NG}{}^{(2)I}(t)$, taking only the $\alpha = 1$ mode into account; (···) shows $g_{NG}{}^{(2)T}(t)$, where $g_{NG}{}^{(2)T}(t) = 0.826[1 + 4D_Tt/\sigma^2]^{-3/2}$, $D_T = 1.18 \times 10^{-13}$ m^2·s^{-1}, and σ is the scattering volume cross section, taken to be 1 μm.

two different experimental geometries are shown; for both experimental geometries the two surfaces are very close to one another, as expected since, at the limit $\epsilon^*/\kappa^* \to 0$, the Harris–Hearst model approximates the Rouse model.

In Figure 6 $g_{NG}{}^{(2)I}(\mathbf{k}_1,\mathbf{k}_2;0)$ for $\mathbf{k}_1 = \mathbf{k}_2 = \mathbf{k}$ is shown as a function of kR_g. (In an experimental setup the detectors would need to be separated by a few degrees[9] so that the contribution of the interference term (eq 1a) to $g^{(2)}$ can be neglected.) For both Rouse and Harris–Hearst models, as $kR_g \to 0$, $g^{(2)I}(0)$ tends to unity and increases monotonically with increasing kR_g. For the Rouse model (as also shown by Pusey[10]) and for the more flexible polymers of the Harris–Hearst type ($\epsilon^*/\kappa^* = 0.001$ and 0.01) $g_{NG}{}^{(2)I}(0)$ reaches a saturating value of 2 at large kR_g ($kR_g \geq 10$). For the stiffer polymer coils our results do not show this saturating behavior. As shown in Figure 2, as the stiffness increases, the number of statistical segments, γL, in the polymer structure decreases, and for $\epsilon^*/\kappa^* = 0.1$, $\gamma L = 1.26$. The value for $g_{NG}{}^{(2)I}(0)$ at $kR_g = 10$ for $\epsilon^*/\kappa^* = 0.1$ is 2.2. Where there are so few statistical segments in the polymer, the Gaussian limit, which would give rise to a saturation value of $g_{NG}{}^{(2)I} = 2$, is clearly not reached. The method described here for calculating $g_{NG}{}^{(2)I}$ by using eq 8 is therefore valid only for the Rouse model and, apparently, for two of the values of ϵ^*/κ^* used here, 0.001 or 0.01.

The remaining figures show properties of the decay curves of $g_{NG}{}^{(2)I}(\mathbf{k}_1,\mathbf{k}_2;t)$, where $\mathbf{k}_1 = \mathbf{k}_2$, with time. In Figure 7 the same normalized cross-correlation function employed by Kam and Rigler[9] (who measured the intensity cross correlation in experiments where $\mathbf{k}_1 \simeq \mathbf{k}_2$), $(g_{NG}{}^{(2)I}(\mathbf{k},\mathbf{k};t) - 1)/(g_{NG}{}^{(2)I}(\mathbf{k},\mathbf{k};0) - 1)$, is plotted against $t(kR_g)^2$ for the Rouse model for $kR_g = 4$, 6, and 8. The points lie on very similar curves. Pusey[10] has discussed the initial slope of the decay,

$$\Gamma = \lim_{t\to 0} \frac{d}{dt} \frac{g_{NG}{}^{(2)I}(\mathbf{k},\mathbf{k};t) - 1}{g_{NG}{}^{(2)I}(\mathbf{k},\mathbf{k};0) - 1} \qquad (37)$$

for Rouse chains, and showed that at high kR_g, Γ was dependent on $(kR_g)^4$. Our numerical results indicate an initial decay for $kR_g = 8$ that is faster than suggested by Figure 7, but by the time the normalized cross-correlation function has decayed by 3% of its initial value (at $t(kR_g)^2$ = 0.32 ms) the differences between the three curves are no longer apparent.

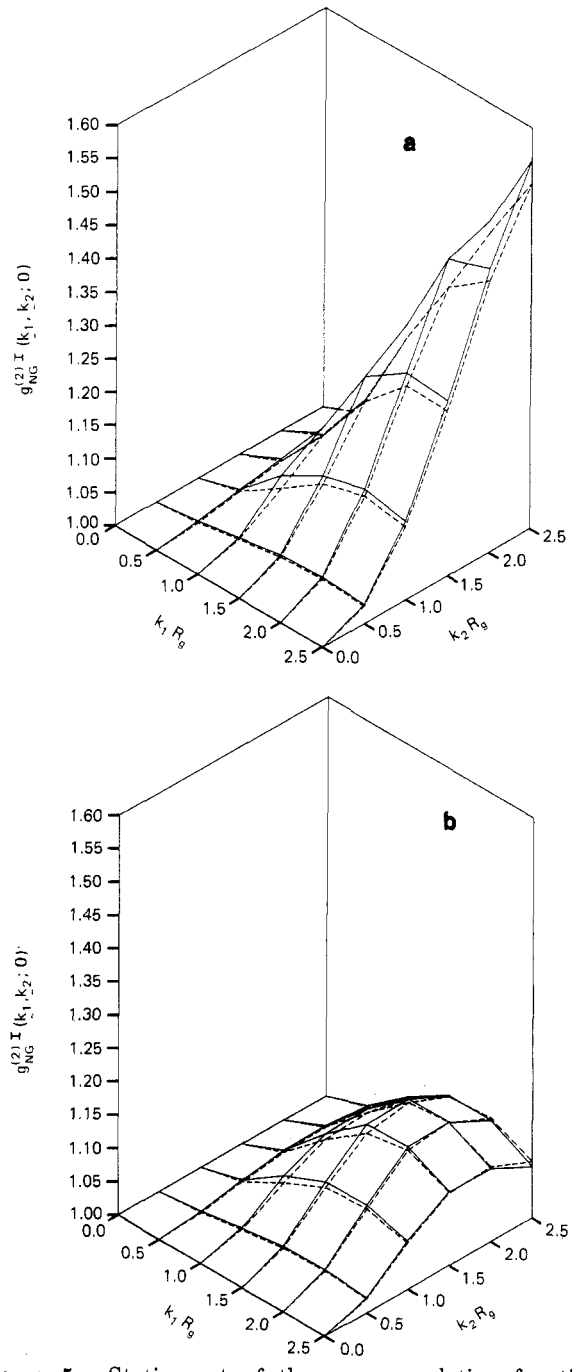

Figure 5. Static part of the cross-correlation function, $g_{NG}{}^{(2)I}(\mathbf{k}_1,\mathbf{k}_2;0)$, calculated from eq 8 for a polymer of $R_g = 193.3$ nm and light of wavelength $\lambda = 451$ nm for the Rouse model (----) and for the Harris–Hearst model for $\epsilon^*/\kappa^* = 0.001$ (—): (a) data for the geometry of Figure 1b; (b) data for the geometry of Figure 1c.

The numerical calculation based on the series expansion as given in eq 19 shows that the decay of the cross correlation is dominated by the first mode for $kR_g \leq 0.8$ (see above). The decay curves, at all values of $kR_g \gtrsim 1$ are multiexponential. Because of the similarity of the shapes of the curves at $kR_g \geq 4$ (Figure 7), we have arbitrarily defined a characteristic time for the decay, $\tau_{1/2}$, as the time taken for $g_{NG}{}^{(2)I}(\mathbf{k}_1,\mathbf{k}_2;t) - 1$ to reach $1/e$ of its initial value. Figure 8 shows log $\tau_{1/2}$ plotted against log kR_g. As kR_g increases, $\tau_{1/2}$ decreases, and for $kR_g \geq 4$ the slope of the graph indicates that at high values of kR_g (≥ 4) the decay of the cross-correlation function with time is dependent

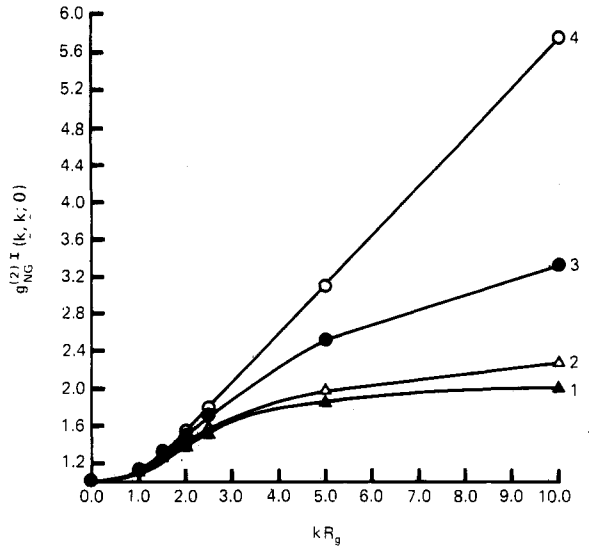

Figure 6. Static part of the cross-correlation function, $g_{NG}^{(2)I}(\mathbf{k}_1,\mathbf{k}_2;0)$ calculated from eq 8 for $\mathbf{k}_1 = \mathbf{k}_2$. Curve 1 shows $g_{NG}^{(2)I}(0)$ for the Rouse model and for the Harris–Hearst model where $\epsilon^*/\kappa^* = 0.001$ and 0.01 (these three curves are indistinguishable on the scale of this graph). Curves 2, 3, and 4 show $g_{NG}^{(2)I}(0)$ for $\epsilon^*/\kappa^* = 0.1$, 1, and 1000, respectively.

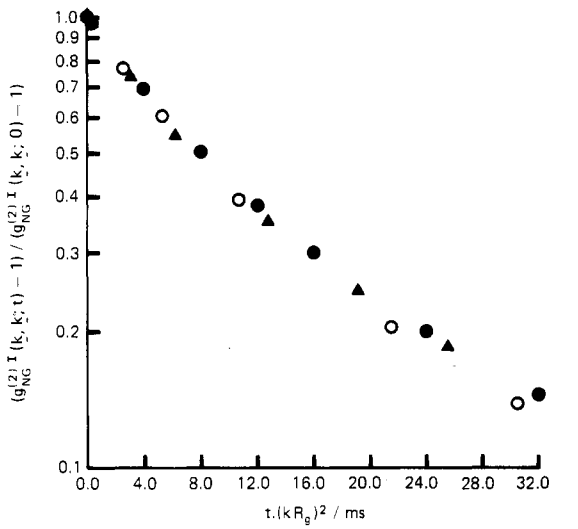

Figure 7. Normalized cross-correlation function, $(g_{NG}^{(2)I}(\mathbf{k},\mathbf{k};t) - 1)/(g_{NG}^{(2)I}(\mathbf{k},\mathbf{k};0) - 1)$ against $t(kR_g)^2$ for $\mathbf{k}_1 = \mathbf{k}_2 = \mathbf{k}$ and $kR_g = 4$ (●), 6 (○), and 8 (▲).

on $(kR_g)^2$, in agreement with the result obtained from Figure 7. Figure 8 also shows curves corresponding to $\tau_{1/2}$ values for the Harris–Hearst model for $\epsilon^*/\kappa^* = 0.001$ and 0.01 for kR_g in the range 1–2.5 (limitations on computing time restricted the range). The decay curves for the Harris–Hearst model also deviate from single exponentiality. The extent of deviation from single exponentiality was characterized by fitting log $(g_{NG}^{(2)I}(t) - 1)$ to a quadratic equation in time:

$$\log [g_{NG}^{(2)I}(t) - 1] = a_0 + a_1 t + a_2 t^2 \qquad (38)$$

Values for a_2/a_1^2 are given in Table II. It may be seen that for the same kR_g, a_2/a_1^2 yields similar values for the Rouse model and for the Harris–Hearst model where $\epsilon^*/\kappa^* = 0.001$. For $\epsilon^*/\kappa^* = 0.01$, a_2/a_1^2 is smaller. This indicates that as the semiflexible polymer becomes stiffer, the relative contributions to the decay from the higher order modes decrease and the decay becomes more like a single exponential. Thus the use of cross correlation involving two detectors at different positions will enable the lower

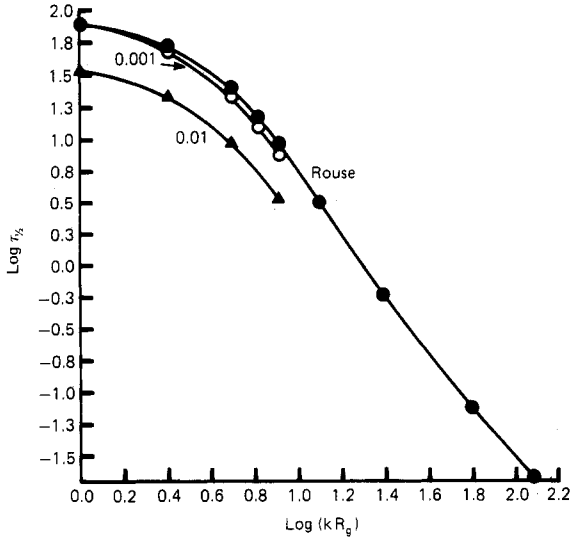

Figure 8. Logarithm of the characteristic time, $\tau_{1/2}$, as defined in the text, for the decay of $g_{NG}^{(2)I}(\mathbf{k},\mathbf{k};t)$, for $\mathbf{k}_1 = \mathbf{k}_2 = \mathbf{k}$, plotted against the logarithm of kR_g for the Rouse model and the Harris–Hearst model, values for ϵ^*/κ^* being annotated.

Table II
Values of a_2/a_1^2 Obtained from Fitting Data Points to the Curve

$$\log (g_{NG}^{(2)I}(\mathbf{k}_1,\mathbf{k}_2;t) - 1) = a_0 + a_1 t + a_2 t^2$$

		Harris–Hearst model, ϵ^*/κ^*	
kR_g	Rouse model	0.001	0.01
1	0.107	0.113	0.083
1.5	0.144	0.149	0.106
2	0.148	0.152	0.115
2.5	0.129	0.126	0.108

order intramolecular modes of a polymer chain to be identified from the short-time decay of $g_{NG}^{(2)I}$, from which information on the flexibility of the chain may be derived.

Comparison of Gaussian Coils with Rods. Let us consider the formula for the first cumulant to $g_{NG}^{(2)I}$ for a Gaussian coil which relates to the experimentally measured initial decay of the correlation function:

$$\left.\frac{\mathrm{d} \log g_{NG}^{(2)I}}{\mathrm{d}t}\right|_{t=0} = -\frac{D_T \mathbf{k}_1\cdot\mathbf{k}_2}{g_{NG}^{(2)I}(\mathbf{k}_1,\mathbf{k}_2;0)} \sum_{ijkl} \exp\left[-\sum_{\alpha}\left[\frac{\langle\mu_\alpha^2\rangle}{6}(k_1^2 Q_{ij\alpha}^2 + k_2^2 Q_{kl\alpha}^2) - \frac{\mathbf{k}_1\cdot\mathbf{k}_2}{3}\langle\mu_\alpha^2\rangle Q_{ij\alpha}Q_{kl\alpha}\right]\right](\delta_{ik} - \delta_{il} - \delta_{jk} + \delta_{jl}) \qquad (39)$$

The 4-fold summation in eq 39 reduces to a 3-fold sum over each of four terms, each consisting of a product of three static correlation functions.

It is clear that when the scattering vectors are such that $\mathbf{k}_1\cdot\mathbf{k}_2 = 0$ the first cumulant for flexible Gaussian coils, given by eq 39, vanishes. Thus the nonvanishing of the first cumulant for wave vectors such that $\mathbf{k}_1\cdot\mathbf{k}_2 = 0$ indicates that the intramolecular dynamics of the scatterers are non-Gaussian; this is clearly the case for a rigid rod for which the $l = 0$ term in the equation for $g_{NG}^{(2)I}$ does not contribute to the first cumulant but the time derivatives of terms with $l \geq 2$ do not vanish for $\mathbf{k}_1\cdot\mathbf{k}_2 = 0$. (It is worth noting that the long-time limit of $g_{NG}^{(2)I}$ for the rod is determined by

$$\lim_{t\to\infty} \sum_{l,\text{ even}} (2l+1)P_l(\cos\Phi)e^{-l(l+1)D_R t}\Lambda_l(k_1,k_2) = \Lambda_0(k_1,k_2) = \sum_{p,q,\text{ even}} I_{pp}(k_1)I_{qq}(k_2) = \langle I(\mathbf{k}_1)\rangle\langle I(\mathbf{k}_2)\rangle \quad (40)$$

which is the expected factorization; this long-time factorization is also obtained from expression 8 for the Gaussian chain.) The forms of eq 8 and 39 apply generally to scattering systems with statistical dynamics described by equations of the form of the Smoluchowski equation (11). Hearst and Harris[22] point out that for large values of the persistence length, their model predicts a dependence of the elastic light scattering form factor on kR_g different from the exact result for a rigid rod scatterer, despite the fact that their calculations constrain the two-point correlation function, $\langle[\mathbf{r}(s) - \mathbf{r}(s')]^2\rangle$, to give the rigid rod result in the limit of infinite rigidity (infinite persistence length). It is interesting to note that this discrepancy, which is a consequence of the use of a Gaussian chain distribution to calculate the form factor, sets in at the same value for γL, the number of statistical segments, as does our observed deviation from Gaussian saturation of $g_{NG}^{(2)I}$.

Clearly, if rodlike behavior (defining a rotational diffusion timescale) takes place in conjunction with chain flexure, then anticorrelations may become apparent, superimposed on higher frequency flexural modes. Crudely, we can assume separation of the rotational diffusion of the rod from its flexural modes and write

$$g_{NG}^{(2)} = g_{NG}^{(2)T}g_{NG}^{(2)I} = g_{NG}^{(2)T}g_{NG}^{(2)F}g_{NG}^{(2)R} \quad (41)$$

where $g_{NG}^{(2)F}$ accounts for contributions to $g_{NG}^{(2)I}$ arising from chain flexure and $g_{NG}^{(2)R}$ is the non-Gaussian cross-correlation function for a rigid rod.

The Harris–Hearst model for a semiflexible polymer, as has been discussed earlier, is not valid for stiffer polymers approaching the limit of rodlike behavior. In the limit of high flexibility, where the chains show Gaussian behavior, the first cumulant, derived from eq 39, vanishes for $\mathbf{k}_1\cdot\mathbf{k}_2 = 0$.

In the case of chain dynamics or colloidal dispersions described by eq 11, exact solutions are available and contain all the information about intrachain/interparticle correlations available from the proposed experiment. For dynamic behavior which is non-Gaussian on the space–time scales defined by the experiment (as with rigid scatterers or, for example, with supramolecular structures consisting of articulated oligomers of rigid rods), where exactly soluble dynamical equations are not available, the analysis of $g_{NG}^{(2)I}$ might show results qualitatively different from the form conjectured in eq 41. We cannot apply our numerical results for large values of the stiffness parameter ($\epsilon^*/\kappa^* \geq 1$) to real systems because (i) the Harris–Hearst model is inadequate to represent chains of great rigidity and (ii) our basic formula for $g_{NG}^{(2)}$ (eq 8) was derived by using the assumption that the chain is adequately represented by a Gaussian chain. Our results for the saturating properties of $g_{NG}^{(2)}(\mathbf{k},\mathbf{k};0)$ provide support for the conclusion of Hearst and Harris[22] that significant deviations from the Gaussian chain property in this model occur as ϵ^*/κ^* changes from 0.01 to 0.1.

We conclude that Gaussian macromolecular chains which give rise to observable decay times in photon correlation experiments for $g_{NG}^{(2)I}$ will be characterized by first cumulants which vanish when $\mathbf{k}_1\cdot\mathbf{k}_2 = 0$. It will be of interest to compare the short-time behavior of cross-correlation functions for a variety of polymers of different flexibility as further experiments are carried out and to look for modulation of the anticorrelation signal in light scattered by slightly flexible rods as a function of wave vectors varying in the region of $\mathbf{k}_1\cdot\mathbf{k}_2 = 0$. The calculation of $g_{NG}^{(2)I}(\mathbf{k}_1,\mathbf{k}_2;t)$ for a flexible rod will be presented elsewhere.

It would also be of considerable interest to attempt to adapt the cross-correlation experiment for use in the study of polymer dynamics in concentrated systems. This might be achieved by modifying refractive index matching techniques so that a small concentration of unmatched polymer dopes a concentrated solution of polymer molecules with refractive index matched to that of the solvent. In this case the number fluctuations would occur on a very long time scale and one scattering (unmatched) polymer molecule could be localized in the small scattering volume for long periods of study. In this way the dynamical effects of entanglement on individual macromolecules could be studied experimentally.

Acknowledgment. We thank C. Bishop and S. P. Weston, of the Institute of Food Research, Reading Laboratory, for assistance with programming and cooperation in provision of considerable CPU time. This work was supported in part by the Agricultural and Food Research Council of Great Britain.

References and Notes

(1) Lin, S.-C.; Schurr, J. M. *Biopolymers* **1978**, *17*, 425.
(2) Fujime, S. *J. Phys. Soc. Jpn.* **1970**, *29*, 751.
(3) Glauber, R. J. *Phys. Rev.* **1963**, *131*, 2766.
(4) Pecora, R. *J. Chem. Phys.* **1968**, *49*, 1032.
(5) Maeda, T.; Fujime, S. *Macromolecules* **1981**, *14*, 809.
(6) Cummins, H. Z.; Carlson, F. D.; Herbert, T. J.; Woods, G. *Biophys. J.* **1969**, *9*, 518.
(7) Fujime, S.; Ishiwata, S.; Maeda, T. *Biophys. Chem.* **1984**, *20*, 1.
(8) Griffin, W. G.; Pusey, P. N. *Phys. Rev. Lett.* **1979**, *43*, 1100.
(9) Kam, Z.; Rigler, R. *Biophys. J.* **1982**, *39*, 7.
(10) Pusey, P. N. *Macromolecules* **1985**, *18*, 1950.
(11) Pusey, P. N. In *Photon Correlation Spectroscopy and Velocimetry*; Cummins, H. Z., Pike, E. R., Eds.; Plenum: New York, 1973.
(12) Yamakawa, H. *Modern Theory of Polymer Solutions*; Harper and Row: New York, 1971.
(13) Zwanzig, R. *Adv. Chem. Phys.* **1969**, *15*, 325.
(14) Soda, K. *J. Phys. Soc. Jpn.* **1973**, *35*, 866.
(15) Moro, K.; Pecora, R. *J. Chem. Phys.* **1978**, *69*, 3254.
(16) Pecora, R. *J. Chem. Phys.* **1965**, *43*, 1562.
(17) Verdier, P. H.; Stockmayer, W. H. *J. Chem. Phys.* **1962**, *36*, 227.
(18) Wang, M. C.; Uhlenbeck, G. E. *Rev. Mod. Phys.* **1945**, *17*, 323.
(19) The denominator of the preexponential factor in the last term of eq 3.8 in ref 10 should be $(X - W)^2(Y - W)^2(X + Y - W)^2$, using Pusey's notation.
(20) This result is based on a form of the Wick Theorem. Doi, M., personal communication.
(21) Harris, R. A.; Hearst, J. E. *J. Chem. Phys.* **1966**, *44*, 2595.
(22) Hearst, J. E.; Harris, R. A. *J. Chem. Phys.* **1967**, *46*, 398.
(23) Hearst, J. E.; Harris, R. A.; Beals, E. *J. Chem. Phys.* **1966**, *45*, 3106.
(24) Using NAG (Numerical Algorithms Group, Oxford, UK) routine E04BBF.
(25) E.g.: Fujime, S.; Maruyama, M. *Macromolecules* **1973**, *6*, 237.
(26) Using NAG routine D01GBF.
(27) Using NAG routine D01FCF.
(28) Using NAG routine D01BCF in conjunction with NAG routine D01FBF.